

DatasetNeRF: Efficient 3D-aware Data Factory with Generative Radiance Fields

Yu Chi^{1,2} Fangneng Zhan² Sibow Wu¹ Christian Theobalt² Adam Kortylewski^{2,3}
 Technical University of Munich¹ Max Planck Institute for Informatics² University of Freiburg³
 {yu.chi, sibow.wu}@tum.de, {fzhan, theobalt, akortyle}@mpi-inf.mpg.de

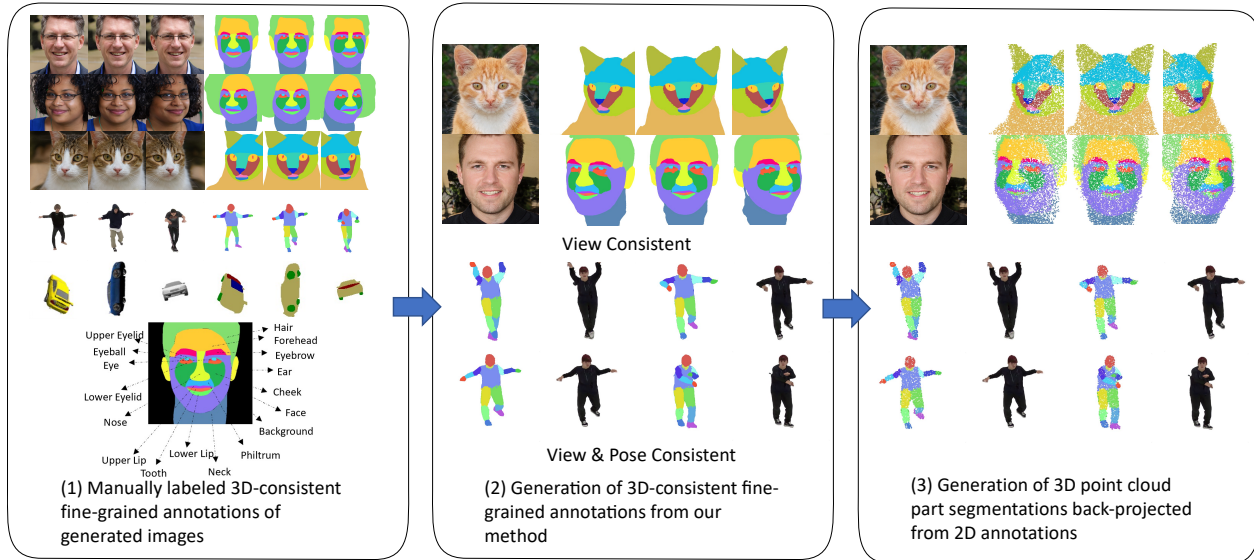


Figure 1. **DatasetNeRF Pipeline Overview:** (1) The manual creation of a small set of multi-view consistent annotations, followed by the training of a semantic segmentation branch using a pretrained 3D GAN backbone. (2) Leveraging the latent space’s generalizability to produce an infinite array of 3D-consistent, fine-grained annotations. (3) Employing a depth prior from the 3D GAN backbone to back-project 2D segmentations to 3D point cloud segmentations.

Abstract

Progress in 3D computer vision tasks demands a huge amount of data, yet annotating multi-view images with 3D-consistent annotations, or point clouds with part segmentation is both time-consuming and challenging. This paper introduces DatasetNeRF, a novel approach capable of generating infinite, high-quality 3D-consistent 2D annotations alongside 3D point cloud segmentations, while utilizing minimal 2D human-labeled annotations. Specifically, we leverage the strong semantic prior within a 3D generative model to train a semantic decoder, requiring only a handful of fine-grained labeled samples. Once trained, the decoder efficiently generalizes across the latent space, enabling the generation of infinite data. The generated data is applicable across various computer vision tasks, including video segmentation and 3D point cloud segmentation. Our approach not only surpasses baseline models in segmentation quality, achieving superior 3D consistency and seg-

mentation precision on individual images, but also demonstrates versatility by being applicable to both articulated and non-articulated generative models. Furthermore, we explore applications stemming from our approach, such as 3D-aware semantic editing and 3D inversion.

1. Introduction

In recent years, research on Large-Scale Models or Foundation Models has become a prevailing trend. Training these kinds of models demands vast amounts of 2D or 3D labeled data, which entails significant human effort. Based on this limitation, a critical question emerges: How do we efficiently generate a substantial volume of high-quality data-annotation pairs while minimizing human labor? Our paper introduces a method to generate an unlimited supply of high-quality, 3D-aware data by utilizing only a limited set of human-provided 2D annotations.

To efficiently scale datasets, several recent approaches [3, 32, 65, 72] utilize rich semantic features from 2D generative models as image representations for downstream tasks, such as semantic segmentation. The remarkable representational capacity of generative models facilitates training segmentation models with only a minimal dataset. During inference, a randomly sampled latent code from the generator is capable of producing a corresponding high-quality annotation. This mechanism effectively transforms the generator into an inexhaustible source of data, enabling the creation of extensive datasets with significantly reduced labeling requirements. However, existing methods predominantly focus on 2D generation models, limiting their capability for 3D-aware tasks. Nevertheless, the emergence of geometry-aware 3D Generative Adversarial Networks (GANs) [7, 8, 49], which decouple latent code and camera pose, offers promising avenues.

In this paper, we introduce *DatasetNeRF*, an efficient 3D-aware data factory based on generative radiance fields. Our 3D-aware Data Factory is adept at creating extensive datasets, delivering high-quality, 3D-consistent, fine-grained semantic segmentation, and 3D point cloud part segmentation as shown in Figure 1. This is accomplished by training a semantic branch on a pre-trained 3D GAN, such as EG3D[8], leveraging the semantic features in the generator’s backbone to enhance the feature tri-plane for semantic volumetric rendering. To improve the 3D consistency of our segmentations, we incorporate a density prior from the pre-trained EG3D model into the semantic volumetric rendering process. We further exploit the depth prior from the pre-trained model, efficiently back-projecting the semantic output to obtain 3D point cloud part segmentation. Our approach facilitates easy manipulation of viewpoints, allowing us to render semantically consistent masks across multiple views. By merging the back-projected point cloud part segmentations from different perspectives, we can achieve comprehensive point cloud part segmentation of the entire 3D representation. Remarkably, our process for generating this vast array of 3D-aware data requires only a limited set of 2D data for training.

We evaluate our approach on the AFHQ-cat[12], FFHQ[26], and AIST++ dataset[33]. We create fine-grained annotations for these datasets and demonstrate that our method surpasses existing baseline approaches, not just in ensuring 3D consistency across video frame sequences, but also in segmentation accuracy for individual images. Additionally, we demonstrate that our method is also seamlessly compatible with articulated generative radiance fields[6] on AIST++ dataset. We also augment the point cloud semantic part segmentation benchmark dataset[68] using our method, with a specific focus on the ShapeNet-Car dataset[9]. Our work further analyzes potential applications like 3D-aware semantic editing and 3D

inversion, demonstrating that the ability to generate infinite 3D-aware data from a limited number of 2D labeled annotations paves the way for numerous 2D and 3D downstream applications.

2. Related Work

Neural Representations and Rendering. In recent years, the emergent implicit neural representation offers efficient, memory-conscious, and continuous 3D-aware representations for objects [2, 20, 41, 50] and scenes [40, 42, 43, 58, 59, 61, 76] in arbitrary resolution. By combining implicit neural representation with volume render, NeRF [42] and its descendants [18, 23, 29, 34, 35, 37–39, 44, 60, 63, 66, 71] have yielded promising results for both 3D reconstruction and novel view synthesis applications. Along with image synthesis, the implicit representations are also used to predict semantic maps [31, 64, 73]. For example, SemanticNeRF [73] augments the original NeRF by appending a segmentation renderer. NeSF [64] learns a semantic-feature grid for semantic maps generation. However, querying properties for each sampled point leads to a low training and inference speed. Considering the pros and cons of explicit representations and implicit representations, recent works [4, 5, 10, 13, 43, 69] propose hybrid representations to complement each other. In this work, we also use hybrid tri-plane representations for 3D modeling.

3D-aware Generative Models. The Generative Adversarial Networks (GANs) [19] have demonstrated remarkable capabilities in generating photorealistic 2D images [16, 25, 27, 28, 70]. With this success, some works extended this setting to 3D domain. For instance, PrGANs [17] and VON [75] first learn to generate a voxelized 3D shape and then project it to 2D. BlockGAN [46] learns 3D features but separates one scene into different objects. However, these approaches encounter challenges in achieving photorealistic details due to the limited grid resolutions.

Recent works [7, 8, 13, 21, 47, 48, 56, 62] integrated neural implicit representation into GANs to enable 3D-aware image synthesis with multi-view consistency. Specifically, GRAF [56] combines NeRF for scene representation with an adversarial framework to enable the training on unposed images; pi-GAN [7] operates in a similar setting but makes some differences in network architecture and training strategy; EG3D [8] learns tri-plane hybrid 3D representation and interprets the aggregated features via volume rendering, ensuring expressive semantic feature extraction and high-resolution geometry-aware image synthesis. While the learned features in generative models are aggregated to generate 3D-aware images, there is still space to harness them for other proposes. In this work, we exploit the possibility of leveraging the learned features from generative NeRF models to generate multi-view-consistent semantic labels along with high-resolution images.

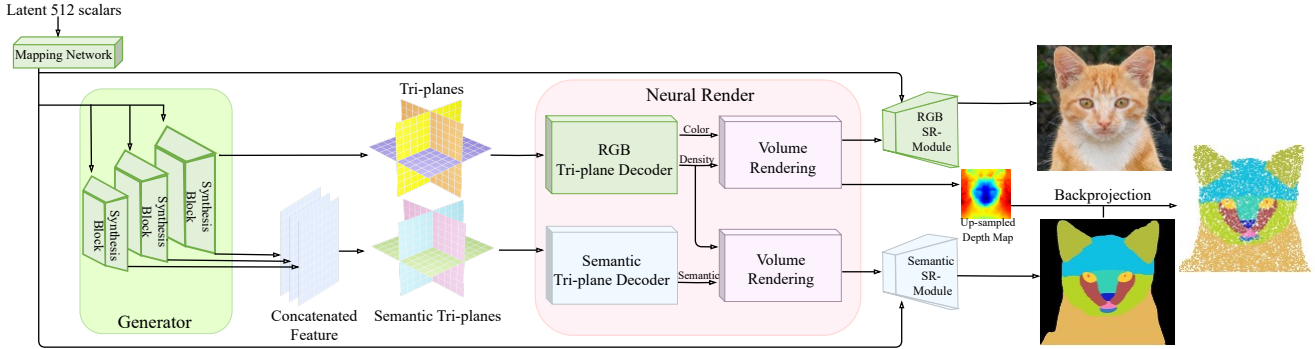


Figure 2. **Overall Architecture of DatasetNeRF.** The DatasetNeRF architecture unifies a pretrained EG3D model with a semantic segmentation branch, comprising an enhanced semantic tri-plane, a semantic feature decoder, and a semantic super-resolution module. The semantic feature tri-plane is constructed by reshaping the concatenated outputs from all synthesis blocks of the EG3D generator. The semantic feature decoder interprets aggregated features from semantic tri-plane into a 32-channel semantic feature for every point. The semantic feature map is rendered by semantic volumetric rendering. We incorporate a density prior from the pretrained RGB decoder during the rendering process to enhance 3D consistency. The semantic super-resolution module then upscales and refines the rendered semantic feature map into the final semantic output. The combination of the semantic mask output and the upsampled depth map from the pretrained EG3D model enables an efficient process for back-projecting the semantic mask, thereby facilitating the accurate generation of point cloud part segmentation.

Synthetic Dataset Generation. Traditional dataset synthesis [15, 51, 54, 55] relies on computer simulations for rendering images along with their corresponding labels, which can greatly save annotation cost. However, models trained on such datasets often face challenges in generalizing to real-world datasets due to domain gaps. Unlike traditional methods of dataset synthesis, the use of generative models for dataset synthesis is favored due to their ability to produce a large number of high-quality and diverse images with similar distribution of natural data [67]. The family of generative models is extensive, with GANs [19], diffusion models [24], and NeRF [42] having achieved notable success in image synthesis. Specifically, many works leverage the rich semantic information learned by GANs to manipulate images [1, 36, 57]. Diffusion models benefit from a stationary training objective and demonstrate decent scalability, enabling the generation of high-quality images [14]. NeRF, as a recent and emerging generative model, has received widespread acclaim for maintaining multi-view consistency. Additionally, the capability of generative models to learn rich semantic information allows such methods to learn to generate new data and labels using only a few manually annotated images [32, 45, 65, 72]. For instance, DatasetGAN [72] leverages StyleGAN [25] as an image generator and synthesize accurate semantic labels with a few human labeled data. Nevertheless, these previous efforts primarily focused on generating semantic maps for 2D datasets. In our work, we leverage StyleGAN2 [27] generator from EG3D [8] to train a semantic decoder, enabling the production of high-quality, 3D-consistent fine-grained semantic segmentation and 3D point cloud part segmentation

with minimal labeled data.

3. Method

We introduce *DatasetNeRF*, a framework designed to generate an extensive range of 3D-aware data. It efficiently produces fine-grained, multi-view consistent annotations and detailed 3D point cloud part segmentations from a limited collection of human-annotated 2D training images.

To address the challenge of generating a varied 3D-aware dataset, we employ a 3D GAN generator as the foundational architecture of our framework. We augment this 3D GAN with a semantic segmentation branch, enabling the production of precise annotations across diverse 3D viewpoints as well as detailed 3D point cloud part segmentations. Figure 2 provides a comprehensive visualization of the entire model architecture. For a more in-depth understanding of the different components of our framework, we delineate the specific backbones used for various tasks in Section 3.1. Subsequently, in Section 3.2, we elaborate on the methodology employed to train the semantic segmentation branch. In Section 3.3, we provide a detailed presentation of both the generation process and the resulting 3D-aware data within the DatasetNeRF framework.

3.1. 3D GAN Generator Backbone

We take EG3D [8] as our backbone model, which introduces a tri-plane architecture for efficient neural rendering at reduced resolutions. This tri-plane consists of reshaped feature representations derived from the output of the generator. To enhance the representational power of the triplane in our work, we take all feature maps $\{S^0, S^1, \dots, S^k\}$

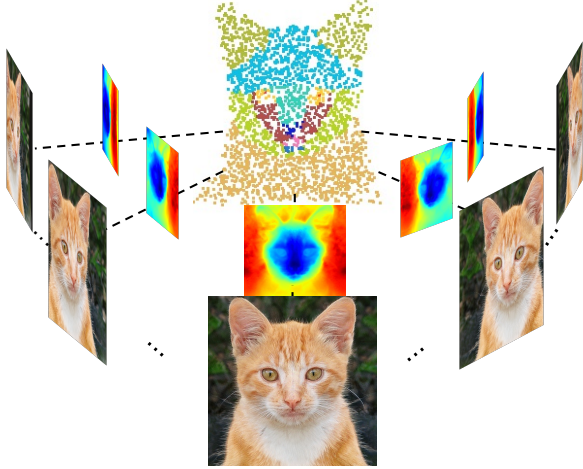


Figure 3. The illustration of multi-view point cloud fusion.

from the the output of consecutive synthesis block of the pretrained generator. These features are upsampled to match the highest output resolution, and subsequently concatenated into a feature tensor with dimensions $[N, N, C]$. Following this, we reshape the concatenated feature tensor into an augmented tri-plane format, similar to that of EG3D[8], to facilitate our semantic neural rendering pipeline. This tri-plane format, distinct from other work[8], represents a key innovation in our work. Its significance and impact are further validated through an ablation study detailed later in the text. Our enhanced tri-plane serves as the semantic feature volume for rendering semantically-rich features within our semantic segmentation branch, enabling accurate depiction of complex structures in images.

Notably, our methodology also exhibits compatibility with a range of 3D GAN architectures, whether articulated or inarticulated. This adaptability underscores the robustness of our approach in generating 3D-consistent segmentation. It facilitates not only multi-view consistency but also pose-consistency in segmentations, further proving the utility of our approach across diverse tasks.

3.2. Semantic Segmentation Branch Training

We query any 3D position x within our semantic tri-plane with enhanced format by projecting it onto each of the three feature planes, obtaining the respective feature vectors (F_{xy}, F_{xz}, F_{yz}) through bi-linear interpolation. These vectors are then aggregated via summation. This aggregated feature serves as the input to the subsequent semantic decoder, which outputs a 32-channel semantic feature. To harness the 3D consistency inherent in the pretrained EG3D model, we re-use the same density σ as the pretrained RGB decoder at the equivalent tri-plane point. For a majority of our experiments, the semantic feature map is rendered

at a resolution of 128^2 . Through semantic volumetric rendering, we derive a raw semantic map $\hat{I}_s \in \mathbf{R}^{128 \times 128 \times C}$ and a semantic feature map $\hat{I}_\phi \in \mathbf{R}^{128 \times 128 \times 32}$. Subsequently, a semantic super-resolution module U_s is utilized to refine the semantic map into a high-resolution segmentation $\hat{I}_s^+ \in \mathbf{R}^{512 \times 512 \times C}$:

$$\hat{I}_s^+ = U_s(\hat{I}_s, \hat{I}_\phi).$$

For a given ground-truth viewpoint P and corresponding latent code z , we compare the ground-truth semantic mask I_s with our model's output semantic mask using cross-entropy loss, mathematically represented as:

$$\mathcal{L}_{CE}(I_s, \hat{I}_s^+) = - \sum_{c=1}^C I_{s,c} \log(\hat{I}_{s,c}^+),$$

where $I_{s,c}$ is the binary indicator of the ground-truth class label for class c and $\hat{I}_{s,c}^+$ is the predicted probability of class c for each pixel in the high-resolution output.

3.3. DatasetNeRF as 3D-aware Data Factory

DatasetNeRF as Multi-view Consistent Segmentations Factory. Empowered by the geometric priors derived from 3D GAN, our DatasetNeRF naturally specializes in generating segmentations that maintain consistency across multiple viewpoints. Once trained, the model adeptly produces high-quality semantic segmentations from a randomly sampled latent code paired with any given pose. The generated multi-view consistent images are illustrated in Figure 4. The easy generation of fine-grained, multi-view consistent annotations markedly diminishes the need for human effort.

DatasetNeRF as 3D Point Cloud Segmentation Factory. Initially, we render a depth map using the pretrained RGB branch. The depth maps are generated via volumetric ray marching. This method computes depth by aggregating weighted averages of individual depths along each ray. The depth map is then upsampled to align with the dimensions of the semantic mask, allowing the semantic mask to be back-projected into 3D space. The entire point cloud of the object is formed by merging semantic maps that have been back-projected from various viewpoints, shown in Figure 3. The efficient acquisition of fine-grained 3D point cloud part segmentation significantly reduces the amount of human effort required. The visualization of point cloud part segmentation is illustrated in Figure 1 (3).

Extension to Articulated Generative Radiance Field. We now showcase how our method can also be applied to articulated generative radiance field. Instead of using EG3D, we adopt the generator of GNARF[5] as our backbone. GNARF[5] introduces an efficient neural representation for articulated objects, including bodies and heads, that combines the tri-plane representation with an explicit feature de-

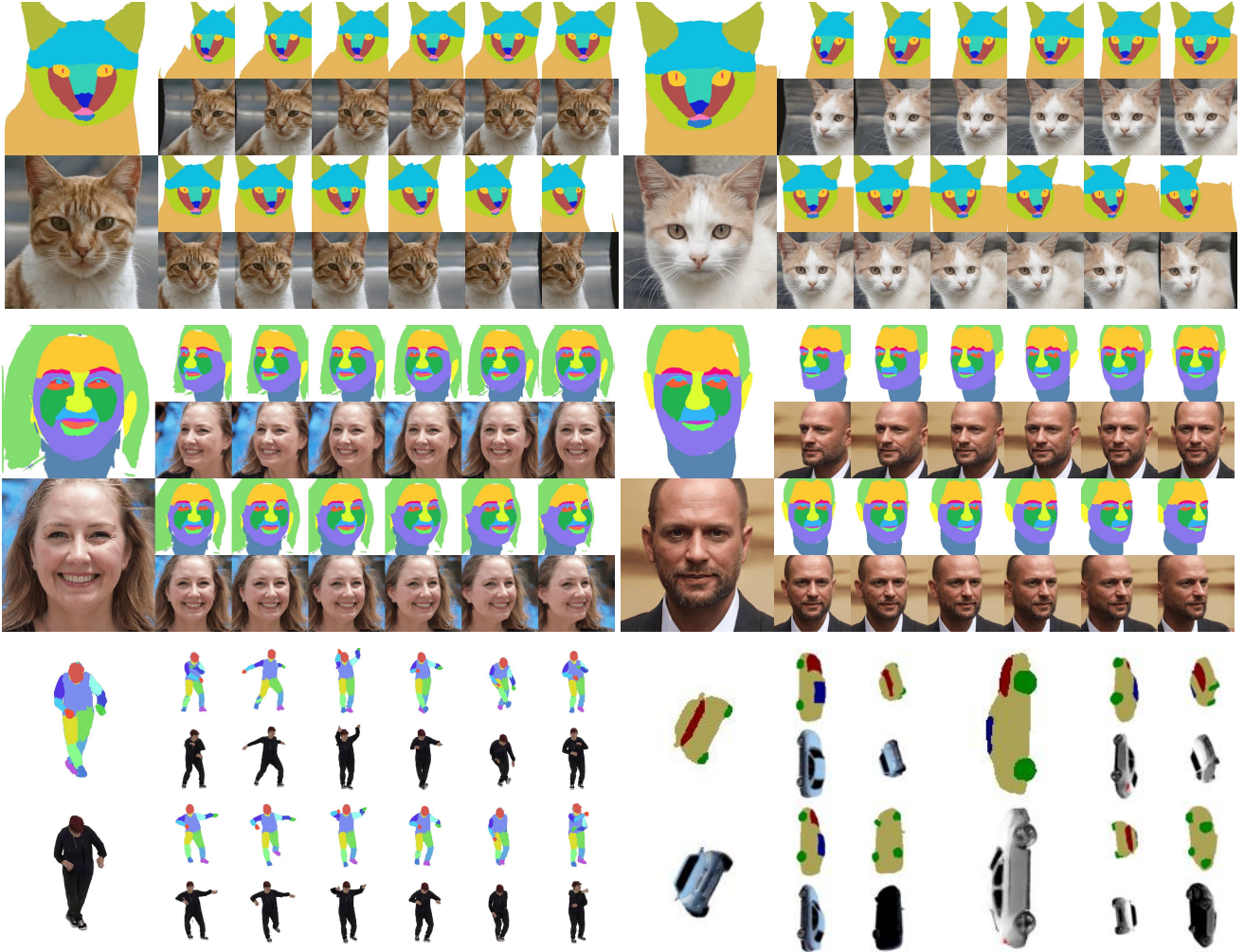


Figure 4. Examples of synthesized image-annotation pairs from our 3D-aware data factory.

formation guided by a template shape. We train our semantic branch on top of the deformation-aware feature tri-plane. The training set contains 150 annotations from 30 different human samples and 60 different training poses. As shown in Figure 4, the result can be well generalized on novel human poses.

4. A Small Dataset with Human Annotations

Our method necessitates a small dataset with annotation. To this end, we employ our backbone model to synthesize a small number of images, followed by a professional annotator for fine-grained annotation. Our fine-grained annotation protocol was applied to AFHQ-Cat [12], FFHQ [26], and AIST++ [33], with a simplified scheme utilized for ShapeNet-Car [9].

Annotation Details For the training set, we crafted 90 different fine-grained annotations for each of the AFHQ-Cat [12] and FFHQ [26] datasets. These encompass 30 dis-

tinct subjects with three different views for each subject. The angular disposition for both training and testing spans from $-\frac{\pi}{6}$ to $\frac{\pi}{6}$ relative to the frontal view, holding all other degrees of freedom constant. Consequently, each subject is depicted in a frontal stance, accompanied by both leftward and rightward poses. The AIST++ dataset [33] posed a greater challenge due to the diversity of human poses, prompting us to generate 150 annotations for 60 disparate poses across a variety of human subjects. With regards to the ShapeNet-Car dataset, our efforts yielded 90 annotations from 30 distinct samples, each from a unique viewpoint. The annotations for ShapeNet-Car, identifying parts like *hood*, *roof*, *wheels*, *other*, align with the standard labels used in the point cloud part segmentation benchmark[68]. The manually created dataset is visualized in Figure 1 (1).

Methods	AFHQ-Cat Ind.		AFHQ-Cat Vid.		FFHQ-Cat Ind.		FFHQ-Cat Vid.	
	mIoU	Acc.	mIoU	Acc.	mIoU	Acc.	mIoU	Acc.
Transfer Learning	0.2995	0.6358	0.2605	0.5766	0.4083	0.7964	0.3895	0.8611
DatasetGAN	0.5381	0.8464	0.5971	0.8625	0.6317	0.8881	0.6390	0.9259
DatasetNeRF	0.6057	0.8798	0.6756	0.9253	0.6200	0.8996	0.6561	0.9278

Table 1. Comparison of different approaches on AFHQ-Cat and FFHQ datasets.

5. Experiments

We conduct extensive experiments with our approach. First, we assess the 2D part segmentation performance across two distinct object categories: cat and human faces. Furthermore, we demonstrate the efficacy of our method in generating 3D point cloud part segmentations for both cat faces and ShapeNet-Cars. Finally, we showcase a variety of 3D applications based on GAN inversion techniques [74].

5.1. 2D Part Segmentation

2D Part Segmentation Network. Consistent with the approach used in DatasetGAN[72], we employ Deeplab-V3[11] with ResNet101[22] backbone as our 2D part segmentation network.

Experimental Setup. Our baselines include transfer learning and DatasetGAN[72]. For the transfer learning approach, we fine-tune the last layer of a pre-trained (on ImageNet) network with our human-annotated data. For the DatasetGAN baseline, we retrain a DatasetGAN model with the annotated data to generate a dataset comprised of 10K image-annotation pairs, which serves as the training set for the Deeplab-V3 segmentation network. We adjust the size of the concatenated feature to match that of the DatasetNeRF’s feature size, ensuring a fair comparison. For our DatasetNeRF, we generate 10K images with uniformly distributed angles which cover both frontal and horizontal views. The Deeplab-V3 segmentation network is then trained from scratch using this dataset. Each test dataset contains 90 unique individual image annotations for arbitrary poses within the training spectrum, as well as a sequential video annotation comprising 61 frames.

Quantitative Evaluation. Table 1 presents the segmentation results for the AFHQ-Cat and FFHQ datasets. In the table, “Ind.” refers to 90 unique individual image annotations representing arbitrary poses within the training range, and “Vid.” denotes a video annotation comprising 61 frames. DatasetNeRF outperforms the baseline models in terms of segmentation quality in the video test set on both AFHQ-Cat and FFHQ datasets. This enhancement underscores the informativeness of the data generated by our approach, which is attributed to the 3D consistency prior inherent from the pretrained generator backbone. Specifically, in the individual test set, DatasetNeRF achieves superior segmen-

tation results for the AFHQ-Cat dataset and demonstrates comparable performance for the FFHQ dataset.

Experiments	Accuracy	mIoU
400 (Generated)	0.8788	0.6268
600 (Generated)	0.8809	0.6447
800 (Generated)	0.8828	0.6403
1100 (Generated)	0.8950	0.6651

Table 2. Training results with different numbers of generated point cloud training samples on AFHQ-Cat dataset.

Experiments	Accuracy	mIoU
600(ShapeNet)	0.8796	0.6773
600(ShapeNet)+725(Generated)	0.9073	0.7519
1325(ShapeNet)	0.9059	0.7412
1325(ShapeNet)+1325(Generated)	0.9104	0.7571

Table 3. Evaluation of the generated point cloud on ShapeNet-Car dataset with PointNet as the backbone model.

5.2. 3D Point Cloud Part Segmentation

We demonstrate the effectiveness of our generated point cloud part segmentation dataset by training PointNet[52] on the generated data. We assess the performance on AFHQ-Cat faces and Shape-Net Car based on mean Intersection-over-Union (mIoU) and accuracy metrics. We show that our approach not only enables the generation of high-quality new point cloud part segmentations dataset from self-annotated 2D images but also acts as a valuable augmentation to existing classical 3D point cloud part segmentation benchmark datasets.

AFHQ-Cat Face Point Cloud Segmentation. From 1200 generated samples, we create a fixed test set of 100 point clouds and train PointNet with varying numbers of training samples. Table 2 illustrates that increased training samples enhance model performance on the test set, which shows the effectiveness of our self-generated point cloud part segmentation dataset.

Augmentation of ShapeNet-Car. Our method’s efficacy,



Figure 5. **3D RGB Inversion.** When presented with an arbitrarily posed input RGB image, our model concurrently optimizes the latent code \mathbf{z} and pose code to develop a 3D representation. It effectively functions as a segmentation model, capable of rendering segmentations from various viewpoints for the given input image.

detailed in Table 3, shows its potential as both a substitute and an augmentation for the original ShapeNet-Car dataset in different experimental setups. The original benchmark dataset consists of 1,825 ShapeNet-Car point cloud part segmentations. Out of these, 500 point clouds are designated as the test set, and the remaining 1,325 serve as the training set.

Settings	mIoU	Accuracy
w/o Multiscale Feature	0.4014	0.7067
w/ Multiscale Feature	0.4796	0.7884
w/o Density Prior	0.4728	0.7813
w/ Density Prior	0.4796	0.7884
w/o Density Prior (Video)	0.6899	0.9188
w/ Density Prior (Video)	0.6913	0.9268

Table 4. Ablation study comparing the impact of different settings on the dataset, focusing on mIoU and accuracy metrics.

Training Samples	AFHQ-Cat Ind.		AFHQ-Cat Vid.	
	mIoU	Acc.	mIoU	Acc.
30 images	0.4394	0.7716	0.6138	0.8892
45 images	0.4588	0.7778	0.6752	0.9148
90 images	0.4795	0.7884	0.6913	0.9268

Table 5. Ablation study on the effect of training sample size on mIoU and accuracy metrics for individual images and video sequences.

5.3. Ablation Study

In this section, we evaluate various aspects of our methodology. We ablate the experiments on AFHQ-Cat dataset. The testset is same as the testset used in Section 5.1. We employ GAN inversion[74] to initially optimize the latent code and pose of an input RGB test image, subsequently generating its corresponding semantic segmentation. We begin by examining the impact of the tri-plane architecture’s size, as

shown in Table 4. Enhancing the original tri-plane architecture from EG3D with multiscale features extracted from the generator’s backbone leads to a significant improvement in performance. Moreover, Table 4 shows incorporating a density prior from the pretrained RGB decoder into the semantic branch is also beneficial. Further, we investigate how the number of training samples affects performance in Table 5. Our findings suggest a moderate improvement when increasing the sample size from 30 to 90 images.

5.4. Applications

We explore a series of applications with our approach, including 3D inversion and 3D-aware editing.

3D RGB Inversion. DatasetNeRF functions effectively as a segmentation model. When given an arbitrary posed RGB image, GAN inversion techniques[74] are employed to jointly optimize the input latent code and pose parameters. The optimized latent code uncovers the underlying 3D structure, thereby allowing for precise rendering of semantic segmentation from multiple viewpoints. The optimization is supervised by MSE loss and Adam[30] optimizer is used. The inversion result is showed in Figure 5.

3D Segmentation Inversion. Pix2pix3D [13] introduces a conditional GAN framework to infer a 3D representation from an input semantic mask. While effective, this approach requires extensive training annotations and significant computational time. DatasetNeRF offers an alternative for accomplishing the similar task. Utilizing an arbitrarily posed semantic mask, our model conducts GAN inversion through its semantic branch. In this process, we jointly optimize the input latent code \mathbf{z} and the pose, employing cross-entropy loss and gradient descent as our optimization strategies. The Adam optimizer[30] is employed in this process. The results of this process are illustrated in Figure 6.

3D-aware Semantic Editing. Our 3D editing system enables users to modify input label maps and subsequently acquire the corresponding updated 3D representation. To accomplish this task, our system focuses on updating the semantic mask output to align with the edited mask while preserving the object’s texture through GAN inversion. Ini-

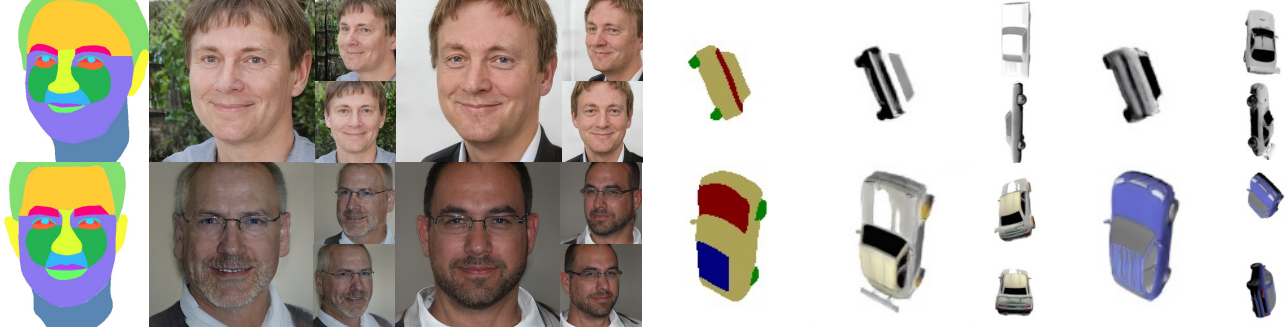


Figure 6. **3D Segmentation Inversion.** Given an arbitrary posed input semantic mask, we jointly optimize the latent code \mathbf{z} and pose code to construct a 3D representation. The inherent 2D-to-3D ambiguity in this process results in a significant diversity in the 3D reconstructions. This optimized representation allows rendering from various viewpoints.



Figure 7. **Semantic Editing Results.** Our 3D editing system enables users to modify input label maps and subsequently acquire the corresponding updated 3D representation. We can render the updated 3D representation from different views.

tially, GAN inversion is employed to determine the initial latent code \mathbf{z} from a given forward-oriented input image, which serves as the starting point for subsequent optimization, enhancing performance. Subsequently, this latent code is refined through GAN inversion to yield the optimized updated representation. We define the region of interest r as a binary mask which includes the union region of the label region before and after the edit. We define the loss function $\mathcal{L}(\mathbf{z}; r)$ to quantify the quality of an edit based on the latent code \mathbf{z} and the region of interest r . It is given by:

$$\begin{aligned} \mathcal{L}(\mathbf{z}; r) = & \lambda_1 \cdot \mathcal{L}_{\text{label}}(G_{\text{semantic}}(\mathbf{z}); M_{\text{edit}}) \\ & + \lambda_2 \cdot \mathcal{L}_{\text{rgb}}(\bar{r} \odot G_{\text{rgb}}(\mathbf{z}); \bar{r} \odot I_{\text{rgb}}) \\ & + \lambda_3 \cdot \mathcal{L}_{\text{vgg}}(\bar{r} \odot G_{\text{rgb}}(\mathbf{z}); \bar{r} \odot I_{\text{rgb}}), \end{aligned}$$

where:

- $G_{\text{semantic}}(\mathbf{z})$ is the rendered semantic mask from \mathbf{z} with the semantic branch G_{semantic} .
- $G_{\text{rgb}}(\mathbf{z})$ is the rendered RGB image with the RGB branch.
- M_{edit} is the edited semantic mask.
- $\mathcal{L}_{\text{label}}$ is the cross-entropy loss for semantic consistency.
- \bar{r} is the complement of the region r .
- \odot is the element-wise product.
- I_{rgb} is the original RGB image.

- \mathcal{L}_{rgb} measures the RGB prediction’s mean squared error.
- \mathcal{L}_{vgg} is the perceptual loss calculated using a VGG-based network.
- $\lambda_1, \lambda_2, \lambda_3$ balance the loss components.

When performing editing on the FFHQ human face dataset, an additional identity loss[53] is incorporated, which calculates the cosine similarity between the extracted features of both the input and edited faces. Figure 7 shows the edited results.

6. Conclusions

We present an efficient and powerful approach to developing a 3D-aware data factory, requiring only a minimal set of human annotations for training. Once trained, the model is capable of generating multi-view consistent annotations and point cloud part segmentations from a 3D representation by sampling in the latent space. Our approach is versatile, compatible with both articulated and non-articulated generative radiance field models, making it applicable for a range of tasks such as consistent segmentation of human body poses. This method facilitates advanced tasks like 3D-aware semantic editing, and 3D inversions including segmentation and RGB inversions. The capability of our model to efficiently produce a wide range

of 3D-aware data from a limited set of 2D labels is not only crucial for training data-intensive models but also opens up new possibilities in various 2D and 3D application domains.

References

- [1] Yuval Alaluf, Omer Tov, Ron Mokady, Rinon Gal, and Amit Bermano. Hyperstyle: Stylegan inversion with hypernetworks for real image editing. In *Proceedings of the IEEE/CVF conference on computer vision and pattern recognition*, pages 18511–18521, 2022. [3](#)
- [2] Matan Atzmon and Yaron Lipman. Sal: Sign agnostic learning of shapes from raw data. In *Proceedings of the IEEE/CVF Conference on Computer Vision and Pattern Recognition*, pages 2565–2574, 2020. [2](#)
- [3] Dmitry Baranchuk, Ivan Rubachev, Andrey Voynov, Valentin Khrulkov, and Artem Babenko. Label-efficient semantic segmentation with diffusion models, 2021. [2](#)
- [4] Miguel Angel Bautista, Pengsheng Guo, Samira Abnar, Walter Talbott, Alexander Toshev, Zhuoyuan Chen, Laurent Dinh, Shuangfei Zhai, Hanlin Goh, Daniel Ulbricht, et al. Gaudi: A neural architect for immersive 3d scene generation. *Advances in Neural Information Processing Systems*, 35:25102–25116, 2022. [2](#)
- [5] Alexander Bergman, Petr Kellnhofer, Wang Yifan, Eric Chan, David Lindell, and Gordon Wetzstein. Generative neural articulated radiance fields. *Advances in Neural Information Processing Systems*, 35:19900–19916, 2022. [2](#), [4](#)
- [6] Alexander W. Bergman, Petr Kellnhofer, Wang Yifan, Eric R. Chan, David B. Lindell, and Gordon Wetzstein. Generative neural articulated radiance fields, 2023. [2](#)
- [7] Eric R. Chan, Marco Monteiro, Petr Kellnhofer, Jiajun Wu, and Gordon Wetzstein. pi-gan: Periodic implicit generative adversarial networks for 3d-aware image synthesis, 2021. [2](#)
- [8] Eric R. Chan, Connor Z. Lin, Matthew A. Chan, Koki Nagano, Boxiao Pan, Shalini De Mello, Orazio Gallo, Leonidas Guibas, Jonathan Tremblay, Sameh Khamis, Tero Karras, and Gordon Wetzstein. Efficient geometry-aware 3d generative adversarial networks, 2022. [2](#), [3](#), [4](#)
- [9] Angel X. Chang, Thomas Funkhouser, Leonidas Guibas, Pat Hanrahan, Qixing Huang, Zimo Li, Silvio Savarese, Manolis Savva, Shuran Song, Hao Su, Jianxiong Xiao, Li Yi, and Fisher Yu. Shapenet: An information-rich 3d model repository, 2015. [2](#), [5](#)
- [10] Anpei Chen, Zexiang Xu, Andreas Geiger, Jingyi Yu, and Hao Su. Tensorf: Tensorial radiance fields. In *European Conference on Computer Vision*, pages 333–350. Springer, 2022. [2](#)
- [11] Liang-Chieh Chen, George Papandreou, Iasonas Kokkinos, Kevin Murphy, and Alan L. Yuille. Deeplab: Semantic image segmentation with deep convolutional nets, atrous convolution, and fully connected crfs, 2017. [6](#)
- [12] Yunjey Choi, Youngjung Uh, Jaejun Yoo, and Jung-Woo Ha. Stargan v2: Diverse image synthesis for multiple domains, 2020. [2](#), [5](#)
- [13] Kangle Deng, Gengshan Yang, Deva Ramanan, and Jun-Yan Zhu. 3d-aware conditional image synthesis. In *Proceedings of the IEEE/CVF Conference on Computer Vision and Pattern Recognition*, pages 4434–4445, 2023. [2](#), [7](#)
- [14] Prafulla Dhariwal and Alexander Nichol. Diffusion models beat gans on image synthesis. *Advances in neural information processing systems*, 34:8780–8794, 2021. [3](#)
- [15] Alexey Dosovitskiy, German Ros, Felipe Codevilla, Antonio Lopez, and Vladlen Koltun. Carla: An open urban driving simulator. In *Conference on robot learning*, pages 1–16. PMLR, 2017. [3](#)
- [16] Zhengcong Fei, Mingyuan Fan, Li Zhu, Junshi Huang, Xiaoming Wei, and Xiaolin Wei. Masked auto-encoders meet generative adversarial networks and beyond. In *Proceedings of the IEEE/CVF Conference on Computer Vision and Pattern Recognition*, pages 24449–24459, 2023. [2](#)
- [17] Matheus Gadelha, Subhansu Maji, and Rui Wang. 3d shape induction from 2d views of multiple objects. In *2017 International Conference on 3D Vision (3DV)*, pages 402–411. IEEE, 2017. [2](#)
- [18] Stephan J Garbin, Marek Kowalski, Matthew Johnson, Jamie Shotton, and Julien Valentin. Fastnerf: High-fidelity neural rendering at 200fps. In *Proceedings of the IEEE/CVF International Conference on Computer Vision*, pages 14346–14355, 2021. [2](#)
- [19] Ian Goodfellow, Jean Pouget-Abadie, Mehdi Mirza, Bing Xu, David Warde-Farley, Sherjil Ozair, Aaron Courville, and Yoshua Bengio. Generative adversarial nets. *Advances in neural information processing systems*, 27, 2014. [2](#), [3](#)
- [20] Amos Gropp, Lior Yariv, Niv Haim, Matan Atzmon, and Yaron Lipman. Implicit geometric regularization for learning shapes. *arXiv preprint arXiv:2002.10099*, 2020. [2](#)
- [21] Jiatao Gu, Lingjie Liu, Peng Wang, and Christian Theobalt. Stylenerf: A style-based 3d-aware generator for high-resolution image synthesis. *arXiv preprint arXiv:2110.08985*, 2021. [2](#)
- [22] Kaiming He, Xiangyu Zhang, Shaoqing Ren, and Jian Sun. Deep residual learning for image recognition, 2015. [6](#)
- [23] Peter Hedman, Pratul P Srinivasan, Ben Mildenhall, Jonathan T Barron, and Paul Debevec. Baking neural radiance fields for real-time view synthesis. In *Proceedings of the IEEE/CVF International Conference on Computer Vision*, pages 5875–5884, 2021. [2](#)
- [24] Jonathan Ho, Ajay Jain, and Pieter Abbeel. Denoising diffusion probabilistic models. *Advances in neural information processing systems*, 33:6840–6851, 2020. [3](#)
- [25] Tero Karras, Samuli Laine, and Timo Aila. A style-based generator architecture for generative adversarial networks. In *Proceedings of the IEEE/CVF conference on computer vision and pattern recognition*, pages 4401–4410, 2019. [2](#), [3](#)
- [26] Tero Karras, Samuli Laine, and Timo Aila. A style-based generator architecture for generative adversarial networks, 2019. [2](#), [5](#)
- [27] Tero Karras, Samuli Laine, Miika Aittala, Janne Hellsten, Jaakko Lehtinen, and Timo Aila. Analyzing and improving the image quality of stylegan. In *Proceedings of the IEEE/CVF conference on computer vision and pattern recognition*, pages 8110–8119, 2020. [2](#), [3](#)

- [28] Tero Karras, Miika Aittala, Samuli Laine, Erik Härkönen, Janne Hellsten, Jaakko Lehtinen, and Timo Aila. Alias-free generative adversarial networks. *Advances in Neural Information Processing Systems*, 34:852–863, 2021. 2
- [29] Petr Kellnhofer, Lars C Jebe, Andrew Jones, Ryan Spicer, Kari Pulli, and Gordon Wetzstein. Neural lumigraph rendering. In *Proceedings of the IEEE/CVF Conference on Computer Vision and Pattern Recognition*, pages 4287–4297, 2021. 2
- [30] Diederik P. Kingma and Jimmy Ba. Adam: A method for stochastic optimization, 2017. 7
- [31] Amit Pal Singh Kohli, Vincent Sitzmann, and Gordon Wetzstein. Semantic implicit neural scene representations with semi-supervised training. In *2020 International Conference on 3D Vision (3DV)*, pages 423–433. IEEE, 2020. 2
- [32] Daiqing Li, Huan Ling, Seung Wook Kim, Karsten Kreis, Adela Barriuso, Sanja Fidler, and Antonio Torralba. Big-datasetgan: Synthesizing imagenet with pixel-wise annotations, 2022. 2, 3
- [33] Ruilong Li, Shan Yang, David A. Ross, and Angjoo Kanazawa. Ai choreographer: Music conditioned 3d dance generation with aist++, 2021. 2, 5
- [34] Kai-En Lin, Yen-Chen Lin, Wei-Sheng Lai, Tsung-Yi Lin, Yi-Chang Shih, and Ravi Ramamoorthi. Vision transformer for nerf-based view synthesis from a single input image. In *Proceedings of the IEEE/CVF Winter Conference on Applications of Computer Vision*, pages 806–815, 2023. 2
- [35] David B Lindell, Julien NP Martel, and Gordon Wetzstein. Autoint: Automatic integration for fast neural volume rendering. In *Proceedings of the IEEE/CVF Conference on Computer Vision and Pattern Recognition*, pages 14556–14565, 2021. 2
- [36] Huan Ling, Karsten Kreis, Daiqing Li, Seung Wook Kim, Antonio Torralba, and Sanja Fidler. Editgan: High-precision semantic image editing. *Advances in Neural Information Processing Systems*, 34:16331–16345, 2021. 3
- [37] Lingjie Liu, Jiatao Gu, Kyaw Zaw Lin, Tat-Seng Chua, and Christian Theobalt. Neural sparse voxel fields. *Advances in Neural Information Processing Systems*, 33:15651–15663, 2020. 2
- [38] Shaohui Liu, Yinda Zhang, Songyou Peng, Boxin Shi, Marc Pollefeys, and Zhaopeng Cui. Dist: Rendering deep implicit signed distance function with differentiable sphere tracing. In *Proceedings of the IEEE/CVF Conference on Computer Vision and Pattern Recognition*, pages 2019–2028, 2020.
- [39] Li Ma, Xiaoyu Li, Jing Liao, Qi Zhang, Xuan Wang, Jue Wang, and Pedro V Sander. Deblur-nerf: Neural radiance fields from blurry images. In *Proceedings of the IEEE/CVF Conference on Computer Vision and Pattern Recognition*, pages 12861–12870, 2022. 2
- [40] Ricardo Martin-Brualla, Noha Radwan, Mehdi SM Sajjadi, Jonathan T Barron, Alexey Dosovitskiy, and Daniel Duckworth. Nerf in the wild: Neural radiance fields for unconstrained photo collections. In *Proceedings of the IEEE/CVF Conference on Computer Vision and Pattern Recognition*, pages 7210–7219, 2021. 2
- [41] Mateusz Michalkiewicz, Jhony K Pontes, Dominic Jack, Mahsa Baktashmotlagh, and Anders Eriksson. Implicit surface representations as layers in neural networks. In *Proceedings of the IEEE/CVF International Conference on Computer Vision*, pages 4743–4752, 2019. 2
- [42] Ben Mildenhall, Pratul P Srinivasan, Matthew Tancik, Jonathan T Barron, Ravi Ramamoorthi, and Ren Ng. Nerf: Representing scenes as neural radiance fields for view synthesis. *Communications of the ACM*, 65(1):99–106, 2021. 2, 3
- [43] Thomas Müller, Alex Evans, Christoph Schied, and Alexander Keller. Instant neural graphics primitives with a multi-resolution hash encoding. *ACM Transactions on Graphics (ToG)*, 41(4):1–15, 2022. 2
- [44] Thomas Neff, Pascal Stadlbauer, Mathias Parger, Andreas Kurz, Joerg H Mueller, Chakravarty R Alla Chaitanya, Anton Kaplanyan, and Markus Steinberger. Donerf: Towards real-time rendering of compact neural radiance fields using depth oracle networks. In *Computer Graphics Forum*, pages 45–59. Wiley Online Library, 2021. 2
- [45] Quang Nguyen, Truong Vu, Anh Tran, and Khoi Nguyen. Dataset diffusion: Diffusion-based synthetic dataset generation for pixel-level semantic segmentation. *arXiv preprint arXiv:2309.14303*, 2023. 3
- [46] Thu H Nguyen-Phuoc, Christian Richardt, Long Mai, Yongliang Yang, and Niloy Mitra. Blockgan: Learning 3d object-aware scene representations from unlabelled images. *Advances in neural information processing systems*, 33:6767–6778, 2020. 2
- [47] Michael Niemeyer and Andreas Geiger. Giraffe: Representing scenes as compositional generative neural feature fields. In *Proceedings of the IEEE/CVF Conference on Computer Vision and Pattern Recognition*, pages 11453–11464, 2021. 2
- [48] Roy Or-El, Xuan Luo, Mengyi Shan, Eli Shechtman, Jeong Joon Park, and Ira Kemelmacher-Shlizerman. Stylesdf: High-resolution 3d-consistent image and geometry generation. In *Proceedings of the IEEE/CVF Conference on Computer Vision and Pattern Recognition*, pages 13503–13513, 2022. 2
- [49] Roy Or-El, Xuan Luo, Mengyi Shan, Eli Shechtman, Jeong Joon Park, and Ira Kemelmacher-Shlizerman. Stylesdf: High-resolution 3d-consistent image and geometry generation, 2022. 2
- [50] Jeong Joon Park, Peter Florence, Julian Straub, Richard Newcombe, and Steven Lovegrove. DeepSDF: Learning continuous signed distance functions for shape representation. In *Proceedings of the IEEE/CVF conference on computer vision and pattern recognition*, pages 165–174, 2019. 2
- [51] Xavier Puig, Kevin Ra, Marko Boben, Jiaman Li, Tingwu Wang, Sanja Fidler, and Antonio Torralba. Virtualhome: Simulating household activities via programs. In *Proceedings of the IEEE Conference on Computer Vision and Pattern Recognition*, pages 8494–8502, 2018. 3
- [52] Charles R. Qi, Hao Su, Kaichun Mo, and Leonidas J. Guibas. Pointnet: Deep learning on point sets for 3d classification and segmentation, 2017. 6

- [53] Elad Richardson, Yuval Alaluf, Or Patashnik, Yotam Nitzan, Yaniv Azar, Stav Shapiro, and Daniel Cohen-Or. Encoding in style: a stylegan encoder for image-to-image translation, 2021. 8
- [54] Stephan R Richter, Vibhav Vineet, Stefan Roth, and Vladlen Koltun. Playing for data: Ground truth from computer games. In *Computer Vision–ECCV 2016: 14th European Conference, Amsterdam, The Netherlands, October 11–14, 2016, Proceedings, Part II 14*, pages 102–118. Springer, 2016. 3
- [55] German Ros, Laura Sellart, Joanna Materzynska, David Vazquez, and Antonio M Lopez. The synthia dataset: A large collection of synthetic images for semantic segmentation of urban scenes. In *Proceedings of the IEEE conference on computer vision and pattern recognition*, pages 3234–3243, 2016. 3
- [56] Katja Schwarz, Yiyi Liao, Michael Niemeyer, and Andreas Geiger. Graf: Generative radiance fields for 3d-aware image synthesis. *Advances in Neural Information Processing Systems*, 33:20154–20166, 2020. 2
- [57] Yujun Shen, Jinjin Gu, Xiaou Tang, and Bolei Zhou. Interpreting the latent space of gans for semantic face editing. In *Proceedings of the IEEE/CVF conference on computer vision and pattern recognition*, pages 9243–9252, 2020. 3
- [58] Vincent Sitzmann, Michael Zollhöfer, and Gordon Wetzstein. Scene representation networks: Continuous 3d-structure-aware neural scene representations. *Advances in Neural Information Processing Systems*, 32, 2019. 2
- [59] Vincent Sitzmann, Julien Martel, Alexander Bergman, David Lindell, and Gordon Wetzstein. Implicit neural representations with periodic activation functions. *Advances in neural information processing systems*, 33:7462–7473, 2020. 2
- [60] Pratul P Srinivasan, Boyang Deng, Xiuming Zhang, Matthew Tancik, Ben Mildenhall, and Jonathan T Barron. Nerv: Neural reflectance and visibility fields for relighting and view synthesis. In *Proceedings of the IEEE/CVF Conference on Computer Vision and Pattern Recognition*, pages 7495–7504, 2021. 2
- [61] Edgar Sucar, Shikun Liu, Joseph Ortiz, and Andrew J Davison. imap: Implicit mapping and positioning in real-time. In *Proceedings of the IEEE/CVF International Conference on Computer Vision*, pages 6229–6238, 2021. 2
- [62] Jingxiang Sun, Xuan Wang, Yichun Shi, Lizhen Wang, Jue Wang, and Yebin Liu. Ide-3d: Interactive disentangled editing for high-resolution 3d-aware portrait synthesis, 2022. 2
- [63] Matthew Tancik, Vincent Casser, Xinchun Yan, Sabeek Pradhan, Ben Mildenhall, Pratul P Srinivasan, Jonathan T Barron, and Henrik Kretzschmar. Block-nerf: Scalable large scene neural view synthesis. In *Proceedings of the IEEE/CVF Conference on Computer Vision and Pattern Recognition*, pages 8248–8258, 2022. 2
- [64] Suhani Vora, Noha Radwan, Klaus Greff, Henning Meyer, Kyle Genova, Mehdi SM Sajjadi, Etienne Pot, Andrea Tagliasacchi, and Daniel Duckworth. Nesf: Neural semantic fields for generalizable semantic segmentation of 3d scenes. *arXiv preprint arXiv:2111.13260*, 2021. 2
- [65] Weijia Wu, Yuzhong Zhao, Hao Chen, Yuchao Gu, Rui Zhao, Yefei He, Hong Zhou, Mike Zheng Shou, and Chunhua Shen. Datasetdm: Synthesizing data with perception annotations using diffusion models, 2023. 2, 3
- [66] Hao Yang, Lanqing Hong, Aoxue Li, Tianyang Hu, Zhenguo Li, Gim Hee Lee, and Liwei Wang. Conranerf: Generalizable neural radiance fields for synthetic-to-real novel view synthesis via contrastive learning. In *Proceedings of the IEEE/CVF Conference on Computer Vision and Pattern Recognition*, pages 16508–16517, 2023. 2
- [67] Zuhao Yang, Fangneng Zhan, Kunhao Liu, Muyu Xu, and Shijian Lu. Ai-generated images as data source: The dawn of synthetic era. *arXiv preprint arXiv:2310.01830*, 2023. 3
- [68] Li Yi, Vladimir G. Kim, Duygu Ceylan, I-Chao Shen, Mengyan Yan, Hao Su, Cewu Lu, Qixing Huang, Alla Sheffer, and Leonidas Guibas. A scalable active framework for region annotation in 3d shape collections. *SIGGRAPH Asia*, 2016. 2, 5
- [69] Fangneng Zhan, Lingjie Liu, Adam Kortylewski, and Christian Theobalt. General neural gauge fields. In *The Eleventh International Conference on Learning Representations*, 2023. 2
- [70] Fangneng Zhan, Yingchen Yu, Rongliang Wu, Jiahui Zhang, Shijian Lu, Lingjie Liu, Adam Kortylewski, Christian Theobalt, and Eric Xing. Multimodal image synthesis and editing: A survey and taxonomy. *IEEE Transactions on Pattern Analysis and Machine Intelligence*, 2023. 2
- [71] Kai Zhang, Gernot Riegler, Noah Snavely, and Vladlen Koltun. Nerf++: Analyzing and improving neural radiance fields. *arXiv preprint arXiv:2010.07492*, 2020. 2
- [72] Yuxuan Zhang, Huan Ling, Jun Gao, Kangxue Yin, Jean-Francois Lafleche, Adela Barriuso, Antonio Torralba, and Sanja Fidler. Datasetgan: Efficient labeled data factory with minimal human effort, 2021. 2, 3, 6
- [73] Shuaifeng Zhi, Tristan Laidlow, Stefan Leutenegger, and Andrew J Davison. In-place scene labelling and understanding with implicit scene representation. In *Proceedings of the IEEE/CVF International Conference on Computer Vision*, pages 15838–15847, 2021. 2
- [74] Jun-Yan Zhu, Philipp Krähenbühl, Eli Shechtman, and Alexei A. Efros. Generative visual manipulation on the natural image manifold, 2018. 6, 7
- [75] Jun-Yan Zhu, Zhoutong Zhang, Chengkai Zhang, Jiajun Wu, Antonio Torralba, Josh Tenenbaum, and Bill Freeman. Visual object networks: Image generation with disentangled 3d representations. *Advances in neural information processing systems*, 31, 2018. 2
- [76] Zihan Zhu, Songyou Peng, Viktor Larsson, Weiwei Xu, Hujun Bao, Zhaopeng Cui, Martin R Oswald, and Marc Pollefeys. Nice-slam: Neural implicit scalable encoding for slam. In *Proceedings of the IEEE/CVF Conference on Computer Vision and Pattern Recognition*, pages 12786–12796, 2022. 2